Resonant microwave transmission through individual sub-wavelength slits

Chris Lawrence[1], James Suckling[2], Roy Sambles[2]

[1]QinetiQ, Cody Technology Park, Farnborough, U.K. GU14 0LX
[2]School of Physics, University of Exeter, Stocker Road, Exeter, U.K., EX4 6NA

ABSTRACT

It is well established that much more radiation may be transmitted through a set of apertures in a metallic screen than a simple calculation from the transmission through the aperture area alone would predict. There has been substantial debate regarding the exact cause of this enhanced transmission, and confusion over the difference between the behaviour of subwavelength apertures as opposed to subwavelength slits. In this study we have analysed the transmission response of individual *slits*, using microwave radiation to ensure that transmission is in no part due to direct passage through the metal screen itself. A set of resonant transmission peaks is caused by the excitation of standing-wave-coupled surface plasmons in the finite length slit. It is also found that the high but finite value of the metals' conductivity influences the transmission response of such slit channels when they are less than 100 microns in width. Indeed there is a strong decrease in transmitted resonant frequency, remarkably tending to zero as the slit width decreases. In addition we have explored the effect of misalignment of the two metal plates that comprise the slit. This modifies resonant frequencies and transmitted intensities through the changing boundary conditions at the slit ends.

Keywords: Transmission, sub-wavelength aperture, slit, microwave, surface plasmon resonance

1. INTRODUCTION

1.1 Previous work

Researchers have recently expended considerable effort in clarifying the transmission mechanisms that can guide electromagnetic radiation through sub-wavelength channels in structured metallic media. This interest was predominantly inspired by the work of Ebbesen *et al* [1] who demonstrated that surprisingly high transmission efficiencies could be achieved if light was made incident upon an array of sub-wavelength apertures in a metallic screen. The work that has followed has detailed the behaviour of a wide variety of sample geometries, including slits[2,3,4], circular holes[5,6] and textured thin films[7], and – perhaps because of this variety – no single all-encompassing theory has been agreed upon with regard to the mechanisms that drive these processes[8]. However, resonant surface charge oscillations known as surface plasmon polaritons (SPPs) are often invoked in the models that have been proposed.

SPPs occur at a metal/dielectric boundary and comprise charge oscillations together with electromagnetic fields that are strongly localised at the interface, decaying exponentially into both media. On a flat interface the mode is non-radiative

and cannot be coupled to by incident radiation since its phase velocity is always greater than that of a free-space photon[9]. The mode can only interact with electromagnetic radiation if the photon's in-plane momentum is boosted. This process is often accomplished through a periodic array of grooves (i.e. a diffraction grating) that supplies momentum in integer multiples of the grating wave vector $k_g = 2\pi/\lambda_g$ (where λ_g is the repeat period of the grating).

Once the SPP is coupled to it can propagate across the metal surface, probing the substrate with its exponentially attenuated evanescent fields. If the metal takes the form of a suitably thin foil (less than of the order of the skin depth) then these fields may be able to span the structure entirely, exciting a second SPP on the opposite face. Then if the underside of the substrate is similarly structured to the upper side, this second SPP can reradiate the power into the adjacent medium. In this way it is possible to create a transmission channel across the metal. This effect can occur at visible frequencies, but in the microwave regime metals exhibit far higher conductivity values, and hence have, relative to the radiation wavelength, a much smaller skin depth. This means that scaled structures of interest (scaled to the incident wavelength) can be tested in microwave experiments in order to show that the transmitted radiation has been channelled through sub-wavelength apertures and not directly through the metal itself. However, because the surface plasmons at microwave frequencies have very long decay lengths into the dielectric then two surface plasmons on either side of a dielectric channel cut into a metal structure will couple together to form a self-coupled almost plane wave.

The presence of self-coupled SPPs in narrow channels has helped to explain the electromagnetic responses of deeply-grooved non-diffractive metallic gratings[10,11]. Results published by Garcia-Vidal et al[12,13] showed that strongly localised SPPs could produce high field intensities and strong absorptions in structures such as arrays of silver half-cylinders and gold lamellar gratings. Sobnack et al[14] predicted that standing wave self-coupled SPP modes are established within the grooves of a non-diffracting grating as their depth is increased, and a set of reflection minima are expected. In addition, Tan et al[15]. have studied the dispersion and the field distribution of SPP modes on very short-pitch (non-diffractive) and deep metal gratings both inside and outside the light line, revealing a set of extremely flat bands with coupled SPP modes localised in the narrow grooves.

Whilst all of the previously mentioned work has concentrated upon the reflectivity of various structures, a number of transmission studies have also been presented. For example, Porto et al[2] have published a theoretical study of non-diffracting metallic transmission gratings with very narrow slits and varying depths. This has enabled them to confirm that there are two possible and distinct transmission mechanisms: either the SPPs on faces of the structure may couple through a thin or perforated metal sheet via their evanescent fields (as described above), or the slits in the metal plates act as Fabry-Perot resonators that can efficiently transmit electromagnetic energy through the substrate. In the former case the transmission efficiency is inevitably set by the thickness and permittivity of the metal (making it an unlikely candidate for high transmissivities at microwave frequencies), whilst the Fabry-Perot effect could be applied to far thicker structures. A theoretical study undertaken by Astilean et al[3] demonstrates the near-100% transmission of infrared light through a one-dimensional array of sub-wavelength diameter slits in silver films and shows that this

Fabry-Perot resonance is mediated by coupled SPPs and that (as per the work of Sobnack *et al*[14]. and Tan *et al*[15]) the resultant mode is a standing wave.

The effect of individual slits has been less comprehensively studied, but underpins all of the aforementioned work. This was realised by Takakura[16], who was concerned that the SPP models were incomplete, and failed to explain the way that (for example) the resonant frequencies appear to shift according to the thickness of the metal substrate[1]. By modelling the behaviour of a single slit in a perfect metal screen Takakura demonstrated that individual sub-wavelength slits act as inefficient Fabry-Perot resonators in their own right, and commented that 'a grating acts as an amplifier of those resonances'. Takakura gives the dependence of the shift of the peak frequency upon slit width by the expression:

$$\frac{\lambda_{shift}}{\lambda_{FP}} = \frac{2(W/T)[\ln(\pi W/\lambda_{FP}) - 3/2]}{2(W/T)[\ln(\pi W/\lambda_{FP}) - 1/2] - \pi}$$

<div align="right">*Equation (1)*</div>

in which W is the slit-width, T is the depth and λ_{FP} is the resonant wavelength as predicted by a simple Fabry-Perot model. However the functional form of this equation has not been verified by experiments[4,17,18]

In addition Sobnack *et al*[14] have suggested that there is an important modification to this model that must be taken into account for very narrow slit-widths. In this regime the coupled plasmons become rather less plane-wave in character, being influenced by the skin depth in the metal. This results in both a shift in resonant frequency and the resonances become much broader. Given that the imaginary component of the metal permittivity (ε_i) will dominate at microwave frequencies, their expression for the resonant frequnecy simplifies to

$$f = f_{FP} - \frac{c}{2\sqrt{2}|\varepsilon_i|^{\frac{1}{2}}W\pi}$$

<div align="right">*Equation (2)*</div>

in which f_{FP} is the idealised Fabry-Perot frequency.

1.2 Aims of this study

In this work we have studied the transmissivities of individual slits in an effort to elucidate the fundamental behaviour of the smallest element in an array. It is clear from the work discussed above that periodically spaced slits can provide high transmission efficiencies. This is because they act as a series of coupled resonators that constructively reinforce each other. The behaviour of *individual* apertures has received little attention, presumably because the efficiencies involved are generally far lower unless some form of adjacent surface texture is included[4,5,6]. However these structures need to be studied since they are far more likely to be encountered in industrial applications, particularly as flaws and faults that can potentially impact upon issues of electromagnetic compatibility.

In this study we have attempted to determine how the transmissivity of individual and unadorned slits is influenced by variations in both the slit-width and the front-face alignment of the two metal plates that comprise each slit. Results are compared to the model of Takakura, and explained with reference to the theories of Sobnack *et al* and modelled fully using a finite element package[19]

2. EXPERIMENTAL

2.1 Sample preparation

The waveguide in our experiment was constructed from two highly polished aluminium plates, each measuring approximately 400 mm by 200 mm, and of 19.58 mm thickness (**T**), as illustrated in Figure 1. The polished faces were held parallel, the gap between the two sheets being set and maintained by the use of smooth-sided dielectric spacers. These spacers were positioned so that they lay beyond the incident beam spot, and varied so as to create slit widths **W** that ranged from approximately 15 μm to 1000 μm. (It should be noted that the slit faces of the aluminium plates were machined to a flatness of about 10 μm.)

The effect of shifting one plate with respect to another whilst maintaining the cavity width was also studied (Figure 1B). Initially the plates were perfectly aligned with their faces equidistant from the source (i.e. **S** = 0), but subsequently the plates were slid across each other, creating overhangs at both the incident and exit faces of the slit in incremental shifts of 0.50mm. The maximum shift was of **S** = 4.5mm, reducing the overlapping region of the plates to 15.08mm. Measurements in these cases were taken at three discrete cavity widths: 50 μm, 200 μm and 500 μm.
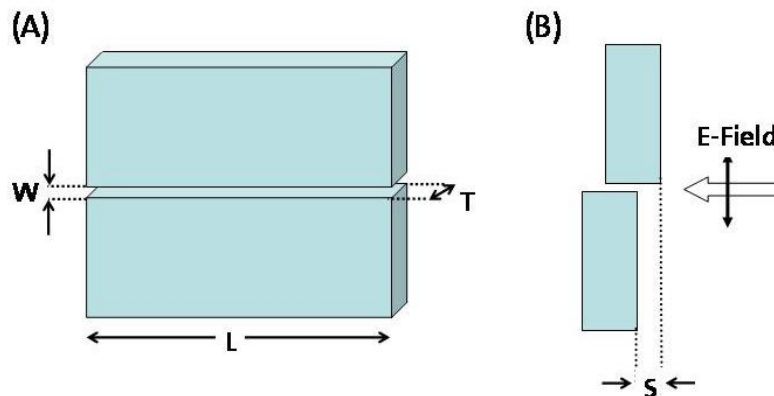

Figure 1: Schematic of the sample geometry: (A) is the front view, and (B) is the side view, including the path and polarization direction of incident radiation.

2.2 Experimental measurements

The slit was placed between two microwave horns, approximately 10cm distant from either. For the radiation wavelengths utilized, the slit was far enough from the source to ensure that the measurements were not made in the near-field region, but close enough to obtain a measurable signal.

The detector was connected to a Hewlett-Packard 87570 scalar network analyser, enabling measurements at wavelengths ranging from 4mm to 20mm (75 GHz to 15 GHz frequency). The horns were set to transmit and receive p-polarised (transverse magnetic, TM) radiation since the system only transmits significant power levels when a component of the electric field lies perpendicular to the plane of the slit.

2.3 Frequency corrections

Due to the finite beam-width of the source, a frequency correction was required for all datasets obtained during these experiments. Whilst perfect (i.e. infinite) plane waves would have no momentum along the slit's length L, this situation is impossible to obtain experimentally. The incident radiation in our experiments is created by a source of finite width, and the Fourier transform of the beam-width at the slit results in an inevitable upward shift in the resonant frequency through the corresponding momentum component. Since our experiments are primarily concerned with the influence of the slit's geometry on the frequency response, it is vital to de-convolve the effect of the incident beam profile.

The dielectric spacers were initially replaced by aluminium elements, effectively creating slits of constrained length **L**. By varying the separation of the aluminium spacers and measuring the transmission through the different-length slits, the effect of a finite beam-width was quantified, producing the graph of Figure 2. This confirms the expected linear relationship between the frequency shift ΔF (from the Fabry-Perot resonant frequency F_{FP}) and the inverse-square of the slit-length **L**:

$$\Delta f \propto \frac{1}{f_{FP} l^2}$$

Equation (3)

The intersection of the line with the y-axis of the graph gives the resonant frequency for an infinitely long slot. This was compared to the value measured with no metal spacers limiting the beam width, and hence the frequency offset due to the finite beam-width was determined. By subtracting this offset value from the experimental data it was possible to compare the results with finite element predictions that presumed plane-wave irradiation Further the size of the shift made it possible to calculate the size of the beam-spot. For example, at a frequency of 68.8 GHz, the N=9 order was shifted by 0.035 GHz, indicating a beam-spot diameter of 68mm; at 15.1 GHz the N=2 order was shifted by 0.019 GHz, and hence a 190mm diameter beam was inferred. The difference in beam diameter is due to differing angular spreads from the different horns that were used to cover the frequency spectrum of interest.
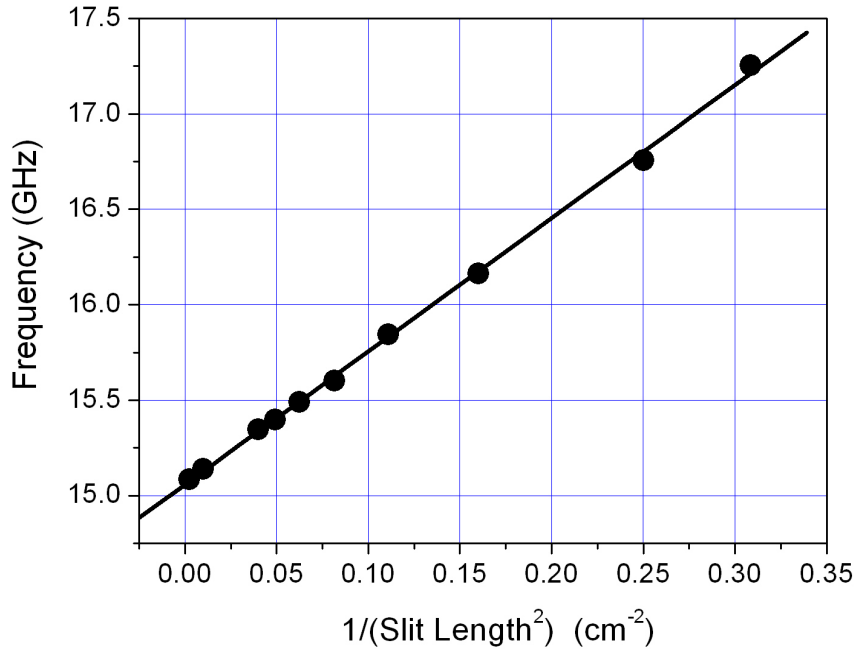
Figure 2: The frequency shifts due to the finite slit length – see text for details.

A second minor correction was also required with regard to the slit width **W**, since there was a slight but unavoidable bowing of the aluminium plates at the centre, reducing the gap. In order to take account of both this and any surface roughness effects it was found that a $10 \pm 4\mu$m reduction in the expected slit width **W** was required.

3. RESULTS & DISCUSSION

3.1 Aligned plates (S=0).

As previously explained, the gap between the two aluminium plates acts as a Fabry-Perot cavity, transmitting a family of wavelengths that meet specific resonant conditions. Figure 3 shows typical datasets for two different slits, one of 500 microns width (i.e. W = 500 μm) and the other of 50 microns width. The frequency plot reveals a series of resonant transmission peaks, of orders starting at N=7 for the lowest frequency (approximately 52GHz for the wider slit). Note the increase in frequency that is introduced by shrinking the slit width by an order of magnitude.
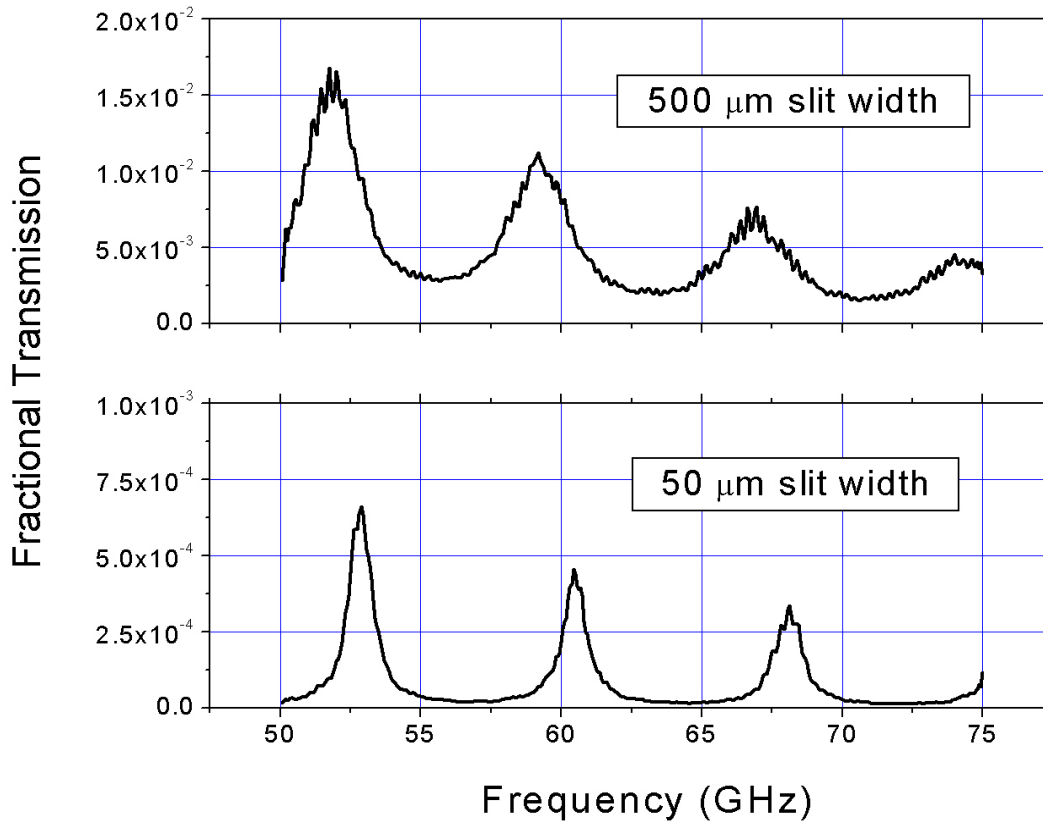
Figure 3: Typical transmission data obtained from zero-offset slits of 50 micron and 500 micron width, revealing a series of resonances at specific frequencies (slightly shifted between the two cases).

The peak transmission for the 7th mode is approximately 1.5% for the larger slit, and roughly 0.06% for the narrower slit. In order to check whether such values are to be expected, we compare the width of the incident beam that strikes the plate surfaces with the area of the slits. Using the beam diameter of 68mm that was previously calculated for radiation at 68.8GHz (see Section 2.3), we estimate that the 500 micron slit occupies approximately 0.9% of the beam area, whilst the 50 micron slit only occupies 0.09%. These two values are comparable to the transmission efficiencies of the peaks nearest to this frequency in the two plots, indicating that these greatly sub-wavelength *individual and unadorned* slits (~1/9th and 1/90th of a wavelength at 66.7GHz) are transmitting ~85% and ~36% of the energy that strikes their entrances, respectively. This is pleasing agreement given that the beam exiting the slits is strongly diffracted (and hence unlikely to be collected in its entirety by the collection horn).
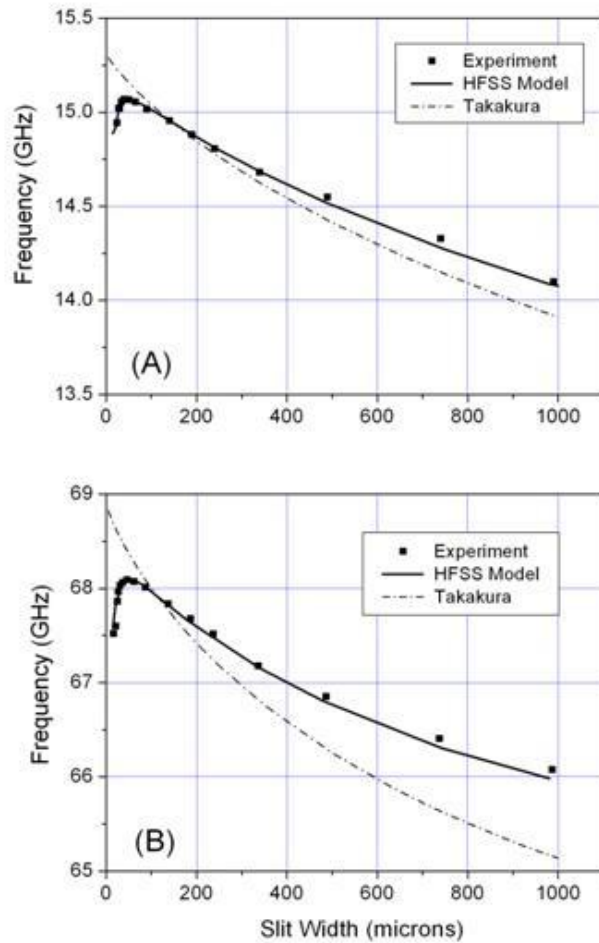
Figure 4: The variation of resonant frequency with slit width for orders (a) N=2, and (b) N=9.

Figure 4 presents transmission data obtained by tracking specific peak orders (N = 2, 9) as the slit-width is varied. The experimental values (indicated by points) reveal a gradual increase in resonant frequency as the slit-width is decreased, in general agreement with the trend of Takakura's model (denoted by the dashed lines). However, there are two problems: firstly, the points do not lie on the dashed lines, indicating quantitative disagreement over the magnitude of the frequency shifts; and secondly, there is a sudden *decrease* in resonant frequency for slit-widths below ~75 μm that is entirely absent from Takakura's model. However, the experimentally-derived datapoints are in excellent agreement with the predictions of a finite element model (Ansoft's High Frequency Structure Simulator (HFSS)[19]), as indicated by the solid lines on the graphs.

The behaviour at low **W** also confirms the predictions of the Preist-Sambles model[14] that takes account of coupled surface plasmon effects at microwave frequencies. This downturn also enables us to determine the imaginary component of the permittivity of aluminium at microwave frequencies, a parameter that now becomes significant in the unusual conditions of a severely sub-wavelength aperture. Our computer models require finite conductivity values **g** for the

metal when calculating the response of our structures, and the Drude model was applied to determine the permittivity using the equation

$$\varepsilon_i = \frac{g}{2\pi\varepsilon_0 f}$$

<div align="right">***Equation (4)***</div>

in which f is the frequency of the incident radiation. This model presumes that the photon frequency is less than the damping constant of the metal (γ) which is of the order of 10^{14} s^{-1} for aluminium: at our microwave frequencies the photon frequency is approximately 10^9 s^{-1}, and hence the condition is admirably well met. At these frequencies it is reasonable to expect the conductivity of bulk aluminium to be comparable to its d.c. (static) value of 3.8 x10^7 S m^{-1}. For the two orders N=2 and N=9 of Figure 4 it is found that the conductivities required to give the solid lines in figure 4 are 3.5 ±0.3 x10^7 S m^{-1} and 1.7 ±0.1 x10^6 S m^{-1}, respectively. (These conductivities result in imaginary permittivity values of ε_I = 4.17 (±0.35) x10^7 at 15.1 GHz, and ε_I = 4.48 (±0.26) x10^6 at 68.1 GHz). Whilst these are in reasonable agreement with the d.c. value, it seems likely that the Drude model cannot be applied in such a simple manner, and that some subtle element of the metal's behaviour is being obscured.

An additional way to examine the frequency shifts is to explore these shifts for a given slit-width as a function of the order N. Figure 5 presents data from the 500 μm slit, comparing experimental results to the predictions of the Takakura model. The frequencies encompassed in this diagram run across the full range of measurements (the peaks being positioned from 15 GHz to 69 GHz). Again, there is a clear disagreement between Takakura's model and the data despite the same trend being exhibited. The shifts are always smallest in the experimental dataset, especially at higher orders in which more wavelengths are contained within the cavity. This substantiates the observation that Takakura's model is incorrect.

Shifting one of the aluminium plates with respect to the other has the fundamental effect of altering the entrance and exit geometries for the cavity. Rather than the waveguide ending in a symmetric 180° opening to air, the region where one plate overlaps another creates a right-angled section at the end of the guide, enabling more complex fields at the entrance (and exit) of the structure. Furthermore, the edge of the prominent plate can diffract the incident radiation, leading to the redirection of power away from the slit, by both direct scattering effects and surface wave excitation. It is hence expected that the introduction of an offset will directly influence both the resonant frequencies and the coupling strengths.
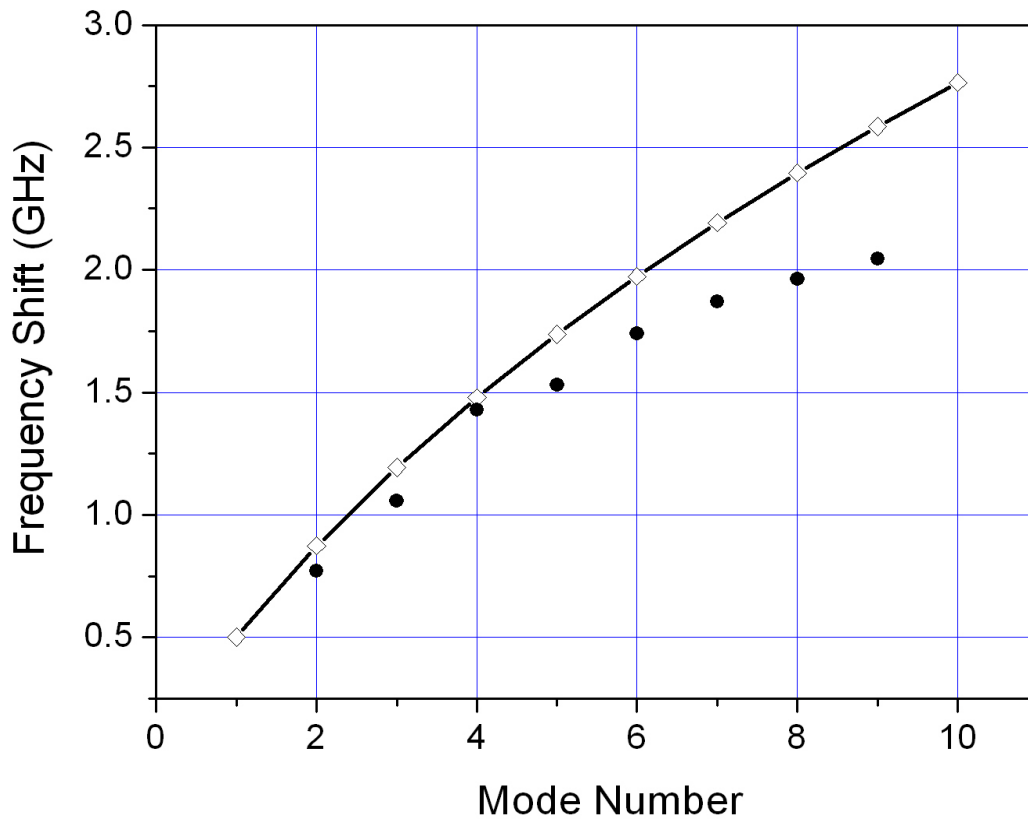
Figure 5: Shifts in resonant frequency from the Fabry-Perot model for different order modes, comparing the predictions of the Takakura model (open symbols and line) with experimental measurements (datapoints).

3.2 Offset plates (S≠0).

Figure 6 presents a single resonant transmission peak (N=7) for the case where **W** = 200 µm, and the offset **S** is varied from 0.0 to 4.0mm. As the offset is introduced there is an almost exponential decrease in the transmission efficiency until **S**>2mm, after which point the intensity is at approximately 20% of the original peak value. There is still a slow degradation of the transmission beyond this point, but it appears that the most pronounced dependence upon **S** is exhibited at small offsets. This behaviour is typical of the situations scrutinised in this study, both experimentally and via model predictions. Note the slight rise in peak transmissivity for the resonance at ~61GHz (i.e. **S** = 3mm). This oscillation in peak values was observed for all modes and slit widths, and is due to the occurrence of constructive interference effects when **S** is equal to an integer multiple of half-wavelengths (although an adjustment is required due to the distorted fields at the slit's ends: 60 GHz radiation corresponds to a wavelength of 5mm., so it would appear that the offset correction corresponds to approximately 0.5mm in this case).
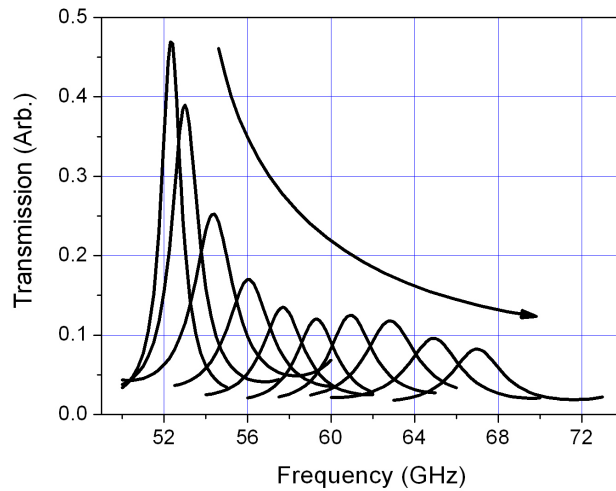
*Figure 6: The transmission of a specific mode (N=8) from a 200 micron width slit, varying the offset distance **S**.
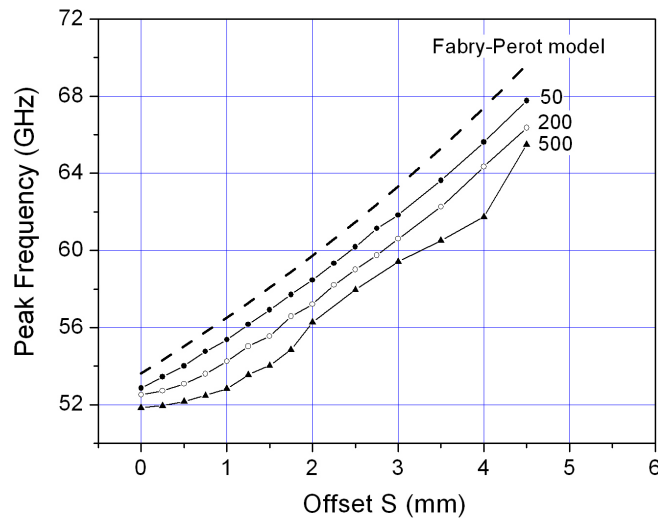Arrow indicates offset increase from 0.0 mm to 4.5 mm, in 0.5mm steps.*

*Figure 7: The dependence of the peak frequency of a specific mode (N=7) upon the offset distance **S**, as compared
to the simple Fabry-Perot model (dashed line). Slits of 50, 200 & 500 microns width are represented*

For Figure 7 data has been obtained from measurements of transmission through slits of 50, 200 and 500 micron width. In each case the peak frequency of the 7th mode is plotted as a function of the offset, and compared to the values expected from a simple Fabry-Perot model. The general trends are the same, with a shift to higher frequencies as the offset increases. This is to be expected, since the depth of the slit defined by parallel regions of the plate is decreasing, and shorter cavities resonate at higher frequencies. However, at short offsets (S < 2 mm) the experimental datasets show far less linear dependence on the offset, exhibiting an almost quadratic dependence for the wider slits.

For the perfectly aligned (i.e. zero offset) plates there is a pronounced impedance mis-match at the entrance and exit of the slit, but a well-defined depth. The channel supports a pseudo-Fabry-Perot mode, with electric field intensity at a maximum at the ends of the plates, and the resonance defined by a series of maxima and minima along the guide.

If S increases then the length of the parallel-plate region obviously decreases by the same amount and hence the peak frequency increases. However, as mentioned above, the entrance and exit of the slit have now been altered, and no longer present the same sharp boundary between waveguide and open-air. This will also affect the resonant frequencies through a change in the field boundary conditions. The field plots in Figure 8 clearly demonstrate this: offset geometries produce distorted fields that extend between the leading edges of both plates, where relatively high-field intensities are to be found. For example, examine the fields when S=0.5mm (Fig.8B): the bright band of high field intensity stretches between the misaligned ends of the plates, suggesting that the effective cavity length now extends beyond the lip of the hindmost plate. This means that the effective cavity depth is *not* simply decreased by the value S, and that there is a more subtle interplay between the frequency shift and the offset. Overall, this effect is of limited influence on the resonant frequency, and its effect will diminish once the two 90° boundaries are far enough apart (of order twice the slit width) to no longer substantially influence the fields in each other's proximities after which further increases in S has little influence upon the field patterns. In other words, this effective lengthening of the cavity provides a minor contribution to the frequency shift that peaks at small offset values with the effect being more pronounced for wider cavities (compare the 50 μm and 500 μm slits in Figure 7) and higher orders.

It is worth noting that our experiments have been restricted to incident angles set parallel to the slit's depth (i.e. normal incidence). At high offset values the leading edge of the foremost plate gives rise to diffractive effects that redirect the incident radiation, and high transmission values cannot be expected at what is effectively a grazing-incidence approach to the cavity's opening. Future work will examine variations in the incident angle, most probably enabling the right-angled cavity to act as a collection horn for the slit.
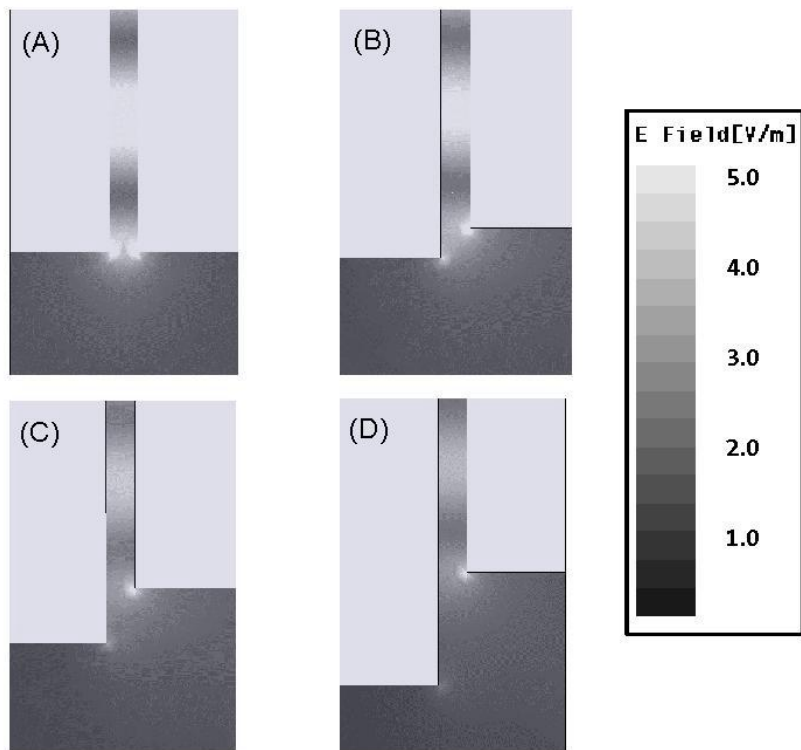
Figure 8. On resonance electric field intensity patterns at the end of a 500 micron width slit, at different offset value: (A) S=0.0mm; (B) S=0.5mm; (C) S=1.5mm; (D) S=2.0mm.

4. CONCLUSIONS

Microwave frequency experimentation is a useful tool for the examination of sub-wavelength aperture effects in metallic structures: the high conductivity of the metal prevents the possibility of field penetration through the metal substrate unless the metal is less than of order the skin depth thick (<<wavelength). Any power transmitted has been directed through the aperture, in this case a slit. Slit apertures support coupled SPP modes which are almost plane waves at this frequency. In the finite length cavity they then set up standing wave states very much like a Fabry-Perot but with large electric fields at the cavity ends. For very thin slits the coupled SPP modes are no longer simple plane waves as boundary condition matching to the fields in the skin depth distort the form of the fields in the cavity. This results in a reduction in the resonant frequencies as the slit is narrowed (the Preist-Sambles effect) and a broadening of the transmission resonances. The nature of this downturn in frequency and mode broadening is dictated by the conductivity of the metal. Thus the naïve treatment that assumes at microwave frequencies that metals are perfect conductors is no longer valid.

We have also shown that the end correction effects for thicker slits does not accord with the Takakura model, although the model does give the correct trend.

Misalignment of the two plates (i.e. the presence of an offset) has the effect of shifting the peak frequencies of the transmission resonances, as would be expected from simple theory. However, any calculation of the exact frequency response must also include the effect of changes to the boundary conditions at the channel's entrance and exit. This alignment issue must be taken into account in any future designs of optical or microwave control devices based upon sub-wavelength apertures (e.g. beam-steerers, polarisers), especially in terms of production tolerances for mass production.

Our findings are of particular relevance to issues of electromagnetic compatibility, since single slits between metallic elements are common features of man-made devices. An example is the airframe of an aeroplane, which exhibits a variety of discontinuities between panels and around doorframes and windows, all of which must be considered with regard to EMC screening[20].

5. ACKNOWLEDGEMENTS

6. REFERENCES

1. T. W. Ebbesen, H. J. Lezec, H. F. Ghaemi, T. Thio and P. A. Wolff, "Extraordinary optical transmission through sub-wavelength hole arrays", Nature **391**, pp. 667-669, 1998.
2. J. A. Porto, F. J. García-Vidal and J. B. Pendry, "Transmission resonances on metallic gratings with very narrow slits", Phys. Rev. Lett. **83**, pp. 2845-2848, 1999.
3. S. Astilean, Ph. Lalanne and M. Palamaru, "Light transmission through metallic channels much smaller than the wavelength", Opt. Commun. **175**, pp. 265-273, 2000.
4. A. P. Hibbins, J. R. Sambles and C. R. Lawrence, "Gratingless enhanced microwave transmission through a subwavelength aperture in a thick metal plate", Appl. Phys. Lett., **81**, pp. 4661-4663, 2002.
5. A. Degiron and T. W. Ebbesen, "Analysis of the transmission process through single apertures surrounded by periodic corrugations", Optics Express, **12**, pp. 3694-3700, 2004.
6. M. J. Lockyear, A. P. Hibbins, J. R. Sambles, and C. R. Lawrence, "Surface-topography-induced enhanced transmission and directivity of microwave radiation through a subwavelength circular metal aperture", Appl. Phys. Lett., **84**, pp. 2040-2042, 2004.
7. S. Wedge and W. L. Barnes, "Surface plasmon-polariton mediated light emission through thin metal films", Optics Express, **12**, pp. 3673-3685, 2004.

8. S. Blair and A. Nahata, "Focus Issue: Extraordinary light transmission through sub-wavelength structured surfaces – Introduction", Optics Express, **12**, pp. 3618, 2004.

9. H. Raether, *Surface Plasmons*, Springer-Verlag, Berlin 1988.

10. R. A. Watts, T. W. Preist and J. R. Sambles, "Sharp surface-plasmon resonances on deep diffraction gratings", Phys. Rev. Lett. **79**, pp. 3978-3981, 1997.

11. J. R. Andrewartha, J. R. Fox and I. J. Wilson, "Further properties of lamellar grating resonance anomalies", Opt. Acta **26**, pp. 197-209, 1979.

12. F. J. García-Vidal and J. B. Pendry, "Collective theory for surface enhanced Raman scattering", Phys. Rev. Lett. **77(6)**, pp.1163-1166, 1996.

13. F. J. García-Vidal, J. Sánchez-Dehesa, A. Dechelette, E. Bustarret, T. López-Rios, T. Fournier and B. Pannetier, "Localized surface plasmons in lamellar metallic gratings", J. Lightwave Tech. **17**, pp.2191-2195, 1999.

14. M. B. Sobnack, W. C. Tan, N. P. Wanstall, T. W. Preist and J. R. Sambles, "Stationary surface plasmons on a zero-order metal grating", Phys. Rev. Lett. **80**, pp. 5667-5670, 1998.

15. W.-C. Tan, T. W. Preist, J. R. Sambles and N. P. Wanstall, "Flat surface-plasmon-polariton bands and resonant optical absorption on short-pitch metal gratings", Phys. Rev. B **59**, pp. 12661-12666, 1999.

16. Y. Takakura, "Optical resonance in a narrow slit in a thick metallic screen", Physics Review Letters, **86**, pp. 5601-5603, 2001.

17. F. Yang and J. R. Sambles, "Resonant transmission of microwaves through a narrow metallic slit", Phys. Rev. Lett., **89**, pp. 063901-4, 2002.

18. J. R. Suckling, A. P. Hibbins, M. J. Lockyear, T. W. Preist, J. R. Sambles and C. R. Lawrence, 'Finite conductance does matter for thin metal slits at microwave frequencies.' Phys. Rev. Lett., **92,**, pp. 147401-4, 2004.

19. High Frequency Structure Simulator, Ansoft Corporation, Pittsburgh, PA, U.S.A

20. J. Carlsson and, P.-S. Kildal, "Transmission through corrugated slots", IEEE Transactions on Electromagnetic Compatibility, 37, pp. 114-121, 1995.